(2)

AR-006-842

MATERIALS RESEARCH LABORATORY
DSTO

Characterization of Deflagrating Munitions by Rotating Prism High Speed Photography

T.J. Kinsey, T.J. Bussell and M. Chick

MRL Technical Report
MRL-TR-91-43

Abstract

We report on the use of a rotating prism high speed camera for determining the characteristics of a munition undergoing rapid deflagration in field experiments. The technique has been applied to study the controlled deflagration of Composition B filled 105 mm shell and 81 mm mortar bombs as representative thick and thin cased munitions respectively; however the report is mostly illustrated with results from the study on 105 mm shell. The deflagration event has been characterized in terms of case expansion rate, initial fragment velocity, time to case burst, time to reaction from the nose end and the deflagration rate of the filling. Products escaping from the fracturing case eventually obscured the image which limited the extent of the measurements.

MATERIALS RESEARCH LABORATORY

Published by

Materials Research Laboratory
Cordite Avenue, Maribyrnong
Victoria, 3032 Australia

Telephone: (03) 246 8111
Fax: (03) 246 8999

AR No. 006-842

APPROVED FOR PUBLIC RELEASE

Authors

T.J. Kinsey

Trevor Kinsey graduated from the Royal Melbourne Institute of Technology, with a Bachelor of Applied Science in Photography in 1981. Since then he has worked at MRL specialising in the field of explosives photoinstrumentation. His principal areas of work in that time have ranged from initiation and detonation studies to fragmentation and ship shock testing.

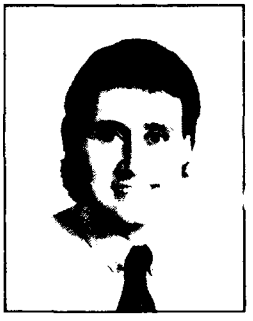

T. Bussell

Tim Bussell studied at the Royal Melbourne Institute of Technology, graduating BAppSc (with Distinction) in Applied Physics. He began work at MRL in 1982 and has been involved in the development and application of various experimental methods to study explosive phenomena. He has had several years experience with flash X-ray systems and is currently developing manganin gauge techniques for application to high pressure measurements in explosives.

M. Chick

Michael Chick graduated as a Licentiate of the Royal Institute of Chemistry (1963). He has worked on explosives research and development for most of his career, commencing at the Atomic Weapons Research Establishment, UK, in 1957 and moving to Explosives Ordnance Division, MRL in 1967. During 1982/83 he was attached to Ballistic Research Laboratory, USA. He is currently concerned with investigating several different aspects of explosives effects; these include the origins of the mass detonation hazard of munitions, the interaction of high velocity metal projectiles with explosives, explosive ordnance disposal and agents neutralization.

Contents

Characterization of Deflagrating Munitions by Rotating Prism High Speed Photography

1. Introduction

An understanding of the consequences of a deflagrating munition will contribute to the assessment of the safety hazard associated with munition transport, storage and disposal.

Mass detonation of ordnance during storage and transport can lead to an enormous loss of life, equipment and facilities. The hazard emanates from a single reacting munition causing detonation of nearby rounds. Original reaction may be caused by a number of stimuli including cookoff, bullet/fragment impact, shaped charge jet strike or electrostatic discharge. Evidence presented by Frey *et al.* [1] and Stosz [2] has shown that mass detonation can result from reactions other than the shocks generated by detonating rounds and Frey and Trimble [3] have demonstrated that some non-detonative reactions can propagate through solid explosives fillings at up to 2.5 km/s in experimental steel, tubular assemblies. Such reaction rates are subsonic and therefore not shocks but may produce the most hazardous effects (fragmentation/ overpressure/adjacent shell projection) next to those produced by a detonation. Thus these reactions may be considered candidates in escalating a non-detonative reaction into a mass detonation. The first step in investigating this proposition is the production and characterization of a controlled deflagration in a munition. We have recently developed a technique that fulfils this role [4]. The method produces a predetermined reaction rate in an explosive filled munition that covers the 2 to 3 km/s range without a transition to detonation occurring.

Characterization of a deflagration also has application in Explosives Ordnance Disposal (EOD), since the aim of some EOD techniques is to burn out the filling leaving the case mainly intact. Ideally this type of event presents no fragmentation and overpressure hazard with important environmental and safety benefits. However, experience has shown that some of these techniques can lead to a rapid deflagration fragmenting the case. For example, our results in applying the Mk 2 Mod 1 Point Focal EOD charge [5] to 105 mm and

155 mm shell have produced violent deflagrations [6]. Thus identification of the features of the deflagrating munition will assist in defining the safety requirements of EOD techniques where a violent deflagration may occur as an unwanted result.

This report describes how rotating prism high speed photography can be applied to determine the characteristics of a munition undergoing a rapid, controlled deflagration in field experiments. The results from a study of Composition B filled 105 mm shell are used to illustrate the technique.

2. *Technique for Producing Controlled Deflagrating Munitions*

The set-up for producing a controlled deflagration of a Composition B filled 105 mm HE shell is shown in Figure 1. In the test the jet was fired through the base of the munition. The MRL 38 mm diameter shaped charge was used in the tests since there is a considerable data base of its effect on munition fillings [7,8]. This shaped charge contains a conventional copper liner with a 42° apex angle. In all tests a witness block was placed under the nose to check that a deflagration was achieved i.e. no indentation is produced by the event. A baffle was incorporated into the assembly to prevent reaction products from the shaped charge from obscuring the image of the shell.

The technique for producing the controlled deflagration of the munition consists of firing the shaped charge jet along the axis of the shell with a velocity below the threshold to produce detonation of the filling. In this way the reaction produced in and behind the bow wave formed in front of the penetrating jet sweeps through the length of the filling leaving no unreacted bulk explosive for a deflagration to detonation transition. Thus it is assumed that the deflagration rate, U_r, is equal to the bow wave velocity U_b. This is supported by flash radiography observations [7,8]. Detonation does not result directly from the bow wave since the pressure-time profile is subcritical. Criteria for the jet initiation of explosive fillings have been discussed in detail elsewhere [7,8].

The jet penetration velocity through the filling is varied by adjusting the thickness of steel interposed between the baffle and the base of the shell. The selected thickness is based on the requirement to erode a sufficient portion of the front of the jet so that the velocity of the tip that enters the filling is at the predetermined value. The method of calculating the thickness of the added steel, x, is described in detail in reference 4 and is summarized below.

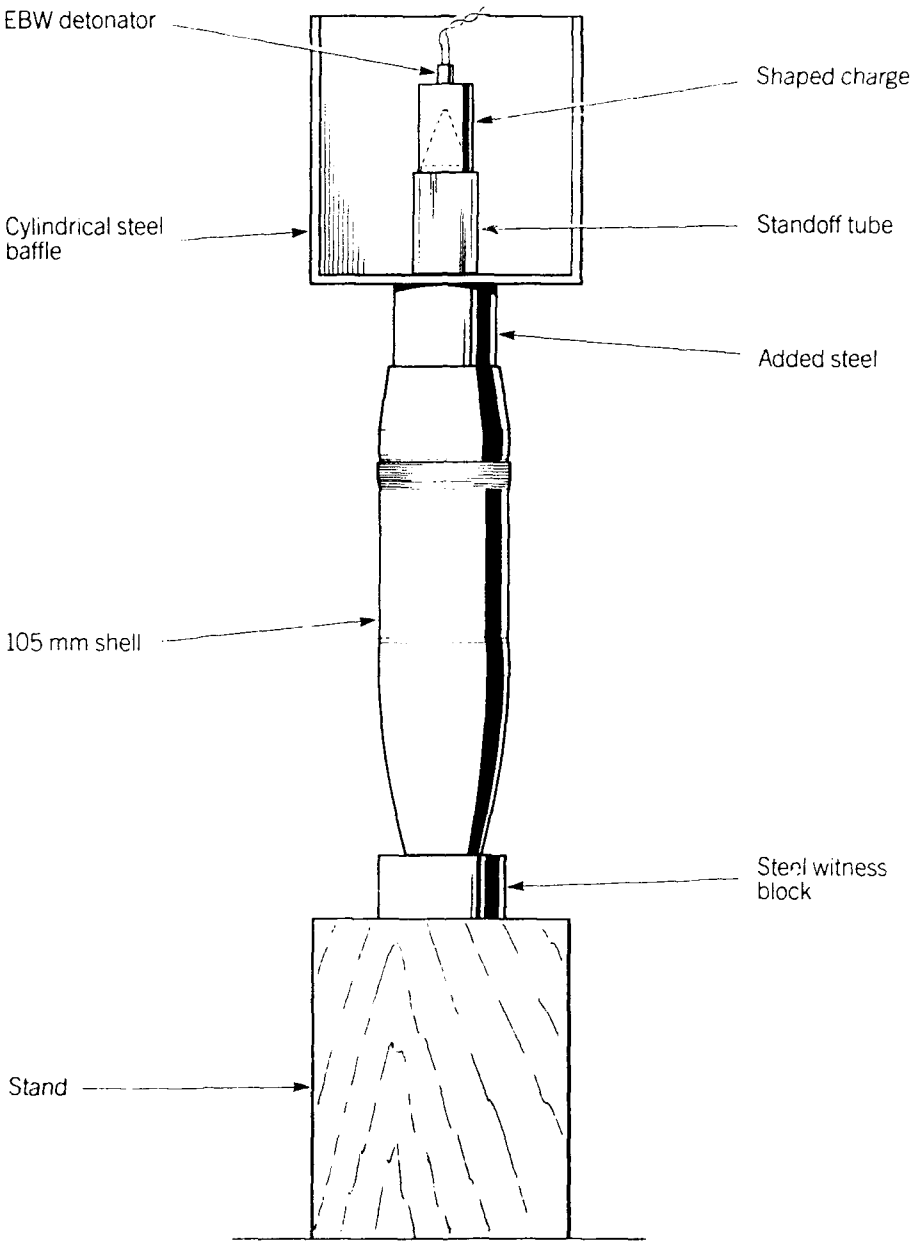

Figure 1: *Experimental set-up for the controlled deflagration of a 105 mm shell.*

Production of the required deflagration rate of 2.5 km/s assumes that the bow wave velocity is equal to the mean jet penetration velocity in the explosive, U_p. Thus,

$$U_r = U_b = U_p = 2.5 \ km/s \tag{1}$$

and from classical penetration theory [9]

$$V_j = U_p (1 + \gamma) \tag{2}$$

where V_j is the jet velocity and γ the square root of the ratio of the target and jet densities. In this case the target is Composition B with a density of 1.65 Mg/m^3 and the jet is copper with a density of 8.9 Mg/m^3; this gives a γ value of 0.430. Thus application of the Dipersio/Simon equation [10] allows back calculation of the jet velocity at the shell case/explosive filling interface, V_j', i.e.

$$V_j = V_j \left[\frac{\tau + s}{s} \right]^{-\gamma} \tag{3}$$

where s is the standoff from the shaped charge virtual origin [11,12] to the shell case/explosive filling interface and τ is the length of the explosive penetrated by the jet. For the system under study τ = 128 mm and s = (119.5 + x) mm, where x is the thickness of added steel. Thus (3) gives V_j' in terms of x.

The value of V_j' is also determined from the jet tip velocity, V_t, and the total thickness of steel penetrated, τ', by the jet in reaching the filling using a modified form of equation (3);

$$V_j = V_t \left[\frac{\tau' + s'}{s' + p} \right]^{-\gamma} \tag{4}$$

where s' is the distance from the virtual origin to the top of the baffle base plate and p is the penetration depth in the steel barrier produced by the cumulative length of the particles which form the constant velocity section at the front of the jet from the 38 mm diameter shaped charge [13]. For these tests p = 10.7 mm for steel, V_t has been measured at 7.4 km/s, s' = 96 mm, τ' = (23.5 + x) mm and the density of the steel baffle and shell case was taken as 7.85 Mg/m^3 giving a value for γ of 0.938.

Thus equating (3) and (4) gives x as the only unknown. For the 105 mm shell under study x was calculated to be 65 mm of steel to give a mean jet penetration velocity and, therefore deflagration rate, of 2.5 km/s.

3. Experimental Details

3.1 Camera

A Redlake Corporation Hycam K2004E rotating prism camera was used to photograph all events. This camera has been extensively modified to suit the conditions encountered in MRL field experiments. These modifications include a remote control facility and on board timing light and event mark generators [14]. The camera was fitted with a quarter frame optical head. This splits each normal 16 mm frame into four, allowing framing rates up to four times that available with a full frame optical head at the expense of frame height. Since one shell was being photographed, the subject suited the modified format when the camera was rotated so that the long axis of the frame was parallel with the axis of the shell. A 1/10 shutter was fitted to the optical head to reduce motion blur. At the framing rates used in the study the exposure time per frame was approximately 2.7 μs.

3.2 Lens

The lens used was a Takumar 500 mm F4.5. This was coupled with a Komura 2X teleconverter to give an effective 1000 mm F9 lens. In each case the lens was used at an effective aperture of F9. This lens combination allowed the camera to be placed at sufficient distance from the charge to reduce the risk of it being hit by a fragment.

3.3 Camera Protection

The camera was sited approximately 100 m from the charge in an aluminium protection box. The end of the box facing the charge was made from steel, with a viewing window made from 25 mm thick laminated glass. The box was designed to allow the camera to be mounted on its side, and a lightweight steel stand was used to raise the box so that the lens axis was 1.5 m above the ground to ensure an unimpeded view of the subject.

3.4 Framing Rate

The camera was powered by a 35 kVA generator situated approximately 75 m from the camera. Previous experience had shown that the voltage drop along the power supply cable prevented high framing rates from being achieved with 30 m film loads. To provide more film for acceleration, and therefore the attainment of higher framing rates, 120 m long film loads were used. The maximum framing rate quoted by Redlake Corporation for a Hycam K2000E camera fitted with a quarter frame head is 44,000 frame/s. Under our field conditions, framing rates of between 35,000 and 40,000 frame/s were achieved.

3.5 *Light Source*

To achieve sufficient exposure at the required high framing rates an inexpensive, expendable light source was provided by an array of Class S flash bulbs back illuminating the subject to provide a silhouette image. Initially shell were illuminated with three Sylvania No. 3 flash bulbs in a vertical line. In later experiments six Sylvania No 3 flash bulbs were used in two lines of three.

The light from the flash bulbs was diffused in two stages to provide even back illumination of the subject. A layer of Roscomat plastic diffusing material was placed 150 mm in front of the flash bulbs and a layer of white tracing paper was placed 150 mm in front of the Roscomat. The whole light source was assembled in a prefabricated stand to aid set-up and alignment. The charge and light source arrangement is shown in Figure 2.

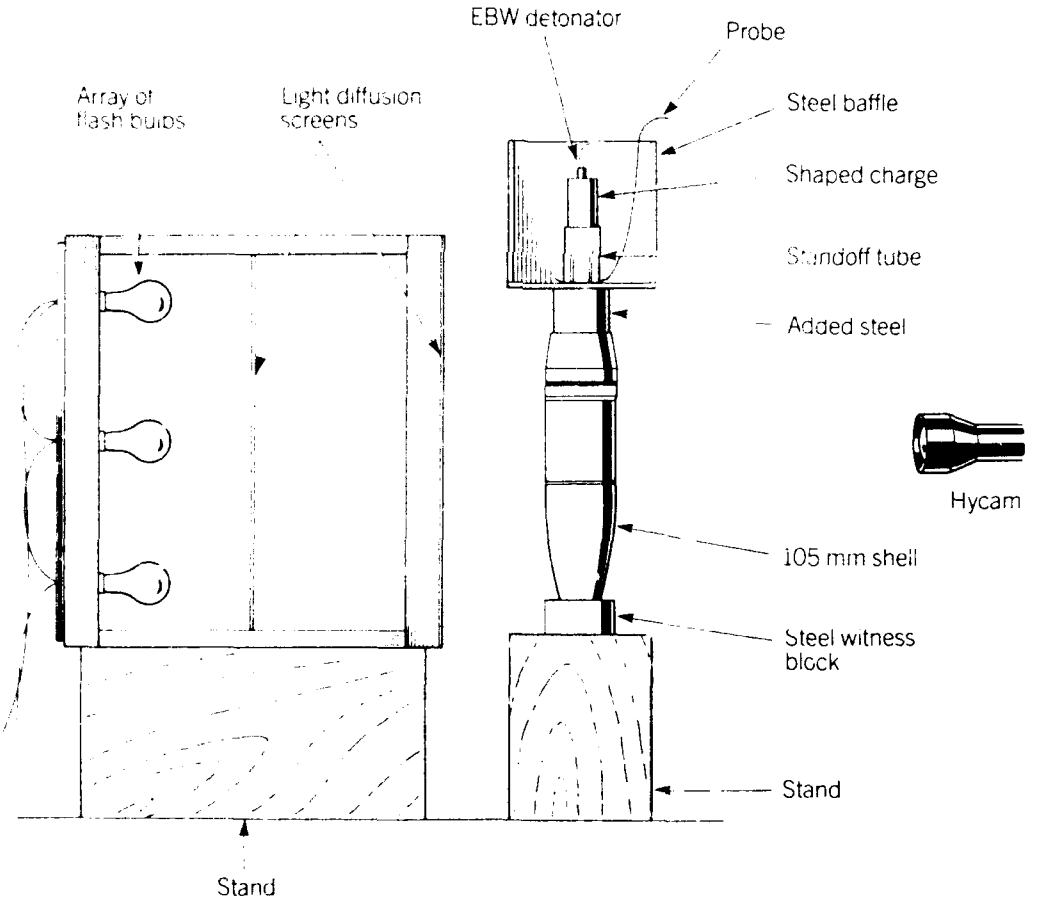

Figure 2: *Light source, subject and camera alignment.*

3.6 *Film and Processing*

Kodak Tri-X Reversal film, emulsion number 7278, was used for all shots. This was processed as a negative in Kodak D-19 developer for 4.5 min at 30°C. This film/developer combination gives a film speed of approximately 160 ASA. The light source, framing rate, shutter factor and lens aperture were selected to give suitable image density with this film speed. Processed films were measured on a Vanguard Instruments motion analyser.

3.7 *Firing Sequence*

Exploding Bridge Wire (EBW) detonators were used to initiate each shaped charge. To ensure that the camera reached operating speed before the detonator was fired, the event switch of the camera was used to trigger the event sequence. The event switch was set to close when 30 m of film remained on the supply spool. This triggered a delayed pulse generator (DPG) which was used to sequence the remaining steps.

The reference time (T_0) output of the DPG was used to trigger an MRL designed flash bulb firing unit [15]. This is a three channel device, with each channel capable of firing several flash bulbs. Each vertical line of flash bulbs was fired by one flash bulb firing unit channel.

After allowing 17 ms for the flash bulbs to reach peak intensity, the DPG triggered an MRL designed EBW firing unit which fired the detonator. A schematic of the wiring is shown in Figure 3.

Simultaneous with the EBW firing unit trigger, the DPG was used to trigger the camera's on board event mark generator. This uses an LED to expose a reference mark on the edge of the film to give a temporal reference for future analysis. As the LED is physically separate from the film gate, the reference mark lags behind the image by five full 16 mm frames (20 quarter frames).

4. *Results and Discussion*

4.1 *Characteristics of a Deflagrating Munition*

The technique has been applied to study the deflagration of Composition B filled 105 mm shell and 81 mm mortar; these were selected as representative thick and thin skinned munitions respectively. Our results from the study on 105 mm shell are used to illustrate the deflagration characteristics of the round although the 81 mm mortar exhibited similar behaviour. Full details of the study using both these munitions and the effects of the deflagration process as a likely source of a mass detonation hazard are presented in references 16 and 17.

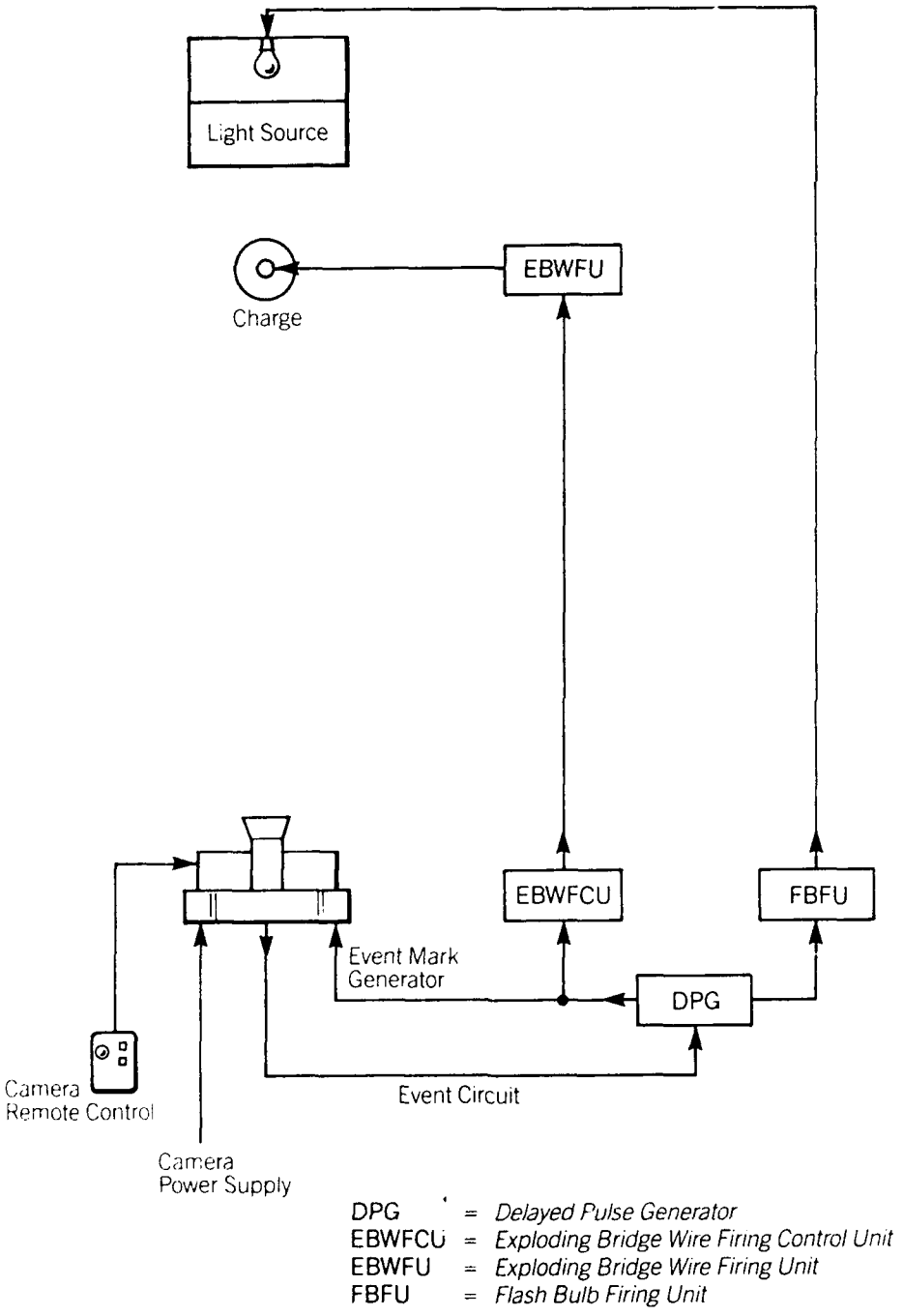

Figure 3: Instrument schematic diagram.

Parameters selected to characterise the deflagrating shell were; expansion rate, fragment velocity, times to case splitting and to reaction from the nose and reaction rate of the filling. Measured values for experiments with 105 mm shell with the nose end plugged and unplugged are given in Table 1. The times listed in Table 1 are from the EBW firing pulse. The times from jet entry into the Composition B filling to the events in Table 1 are 55 μs less than these values; this is the time estimated for the functioning of the shaped charge device and for the jet to travel across the standoff distance and penetrate through the base of the shell. Deflagration commencement was assumed to coincide with jet entry into the filling. Note that a major limit on the accuracy of the times is the interframe time of about 25 μs. Products escaping from the fracturing case eventually obscured the image and this limited the extent of the measurements.

Figures 4 (a) and (b) show a film sequence of deflagrating plugged and unplugged shell respectively. The jet deflagration device was fired from the top of the picture. The baffle around the shaped charge prevents the detonation products from the shaped charge device obscuring the view of the shell. This is followed a few frames later by products escaping from the fracturing case in the region of the driving band and from the unplugged nose in Shot 2. The first sign of the products from case fracture was taken as the onset of case break-up.

Table 1 data show there is variability in the relative occurrence of the events; for example, for the two unplugged rounds light emission from the nose in Shot 2 appears at a similar time to case fracture but precedes case fracture in Shot 1.

Table 1: *Characteristics of the controlled deflagration of Composion B filled 105 mm shell*

Shell Configuration	Time from the Detonator Pulse to Event			Deflagration Propagation Velocity		Maximum Expansion Velocity km/s	Estimated Initial Fragment Velocity km/s
	Initial Case Fracture μs	Products from Nose μs	Image Obscured μs	From Case Expansion Data km/s	Calculated km/s		
Unplugged SHOT 1	440	310	490	2.3	2.5	*Pt 1, 0.24 Pt 2, 0.30 Pt 3, 0.35	Pt 1, 0.12 Pt 2, 0.15 Pt 3, 0.17
Unplugged SHOT 2	460	460	530	2.5	2.5	Pt 1, 0.22 Pt 2, 0.36 Pt 3, 0.22	Pt 1, 0.12 Pt 2, 0.18 Pt 3, 0.11
Plugged SHOT 3	340	470	440	-	2.5	Pt 1, 0.12 Pt 2, 0.08 Pt 3, 0.20	Obsured by Products 0.1 (see text)
Plugged SHOT 4	320	450	370	-	2.5	Obscured by products	
Plugged SHOT 5	320	490	510	2.2	2.5	Pt 1, 0.39 Pt 2, 0.25 Pt 3, 1.96	Pt 1, 0.20 Pt 1, 0.12 Pt 3, 0.98

* Pt represents Points as shown in Figure 6.

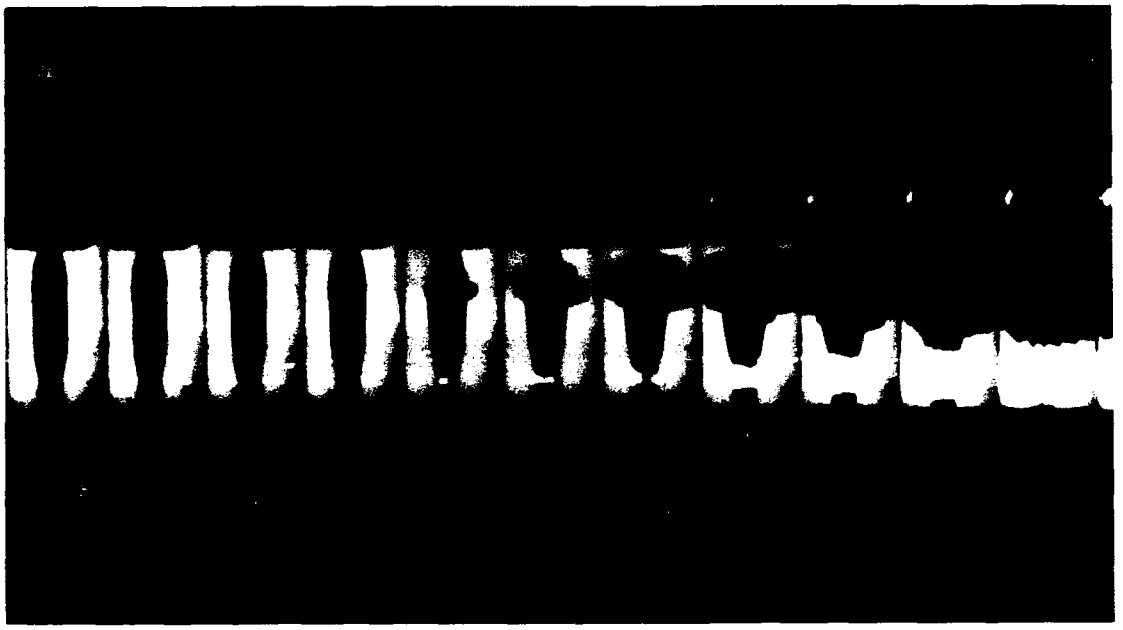

(a)

(b)

Figure 4: *Prints of the camera records showing deflagrating (a) plugged and (b) unplugged 105 mm shell.*

Graphical representation of the shell expansion data measured from the camera records is shown in Figures 5 (a) and (b). The diameter of the expanding shell was measured at three points, see Figure 6. The first point was 120 mm from the base, just below the driving band. The second point was 180 mm from the base near the centre of the shell and the third point was 240 mm from the base, near the fuze cavity. For the unplugged shell in Figure 5 (a) the onset of expansion at points 1, 2 and 3 was 286 μs, 312 μs and 338 μs respectively from the EBW firing pulse. This corresponds to a velocity of 2.3 km/s down the shell and compares with a calculated mean penetration velocity through the length of the filling of 2.5 km/s. The data from Figure 5 (b) follows a similar trend. The data from Shots 1 and 2 in Table 1 suggest that the deflagration swept through the explosive filling before case breakup. Shell expansion prior to breakup was about 30% of the initial diameter (i.e. 15 mm increase in the shell radius).

Within the limitations of experimental error in the measurements in Table 1 caused by the interframe time of about 25 μs, the time to initial case fracture for both the plugged and unplugged rounds and the times to product emission from the nose for the plugged rounds are reasonably consistent. Thus it can be assumed with reasonable confidence that initial case fracture occurred earlier for the plugged than the unplugged rounds suggesting that product pressure build-up may have influenced the process. This in turn influences the interpretation of the case expansion data in terms of the deflagration velocity in the explosive filling. This matter is discussed in more detail in reference 17.

The variations in the times for product emission from the shell nose for the unplugged rounds (Shots 1 and 2, Table 1) may be related to the fit between the shell nose and witness block. A gap will allow prompt product emission and detection whereas a tight fit may not. The lack of such a gap may explain why the time for Shot 2 is similar to that for the plugged rounds. Also we note that there is no indication on any of the films that the deflagration process causes the shell to shift its position which would be expected to produce a path for product emission from between the nose and witness block. Further discussion on these observations is given in reference 17.

Image obscuration times in Table 1 do not appear to be reproducible and this may be at least partly due to the less predictable manner in which direction the products will escape from the splitting case and expand across the camera field of view.

The estimated velocities of fragments given in Table 1 are taken as half the final expansion velocity. On this basis both the unplugged rounds gave values within the 110 to 180 m/s range. In contrast fragments from detonating Composition B 105 mm shell have velocities of about 1.1 km/s [18]. Estimates for points 1 and 2 for Shot 3 and all three points in Shot 4 (the plugged rounds) were not obtained since product obsuration occurred early in the shell expansion process. Comparison of the data for point 3 in Shot 3 to the corresponding curves in Figures 5 (a) and (b) suggest the estimated value (100 m/s) may be low due to product obscuration. Even so the value is close to the lower range of the values for the unplugged shell.

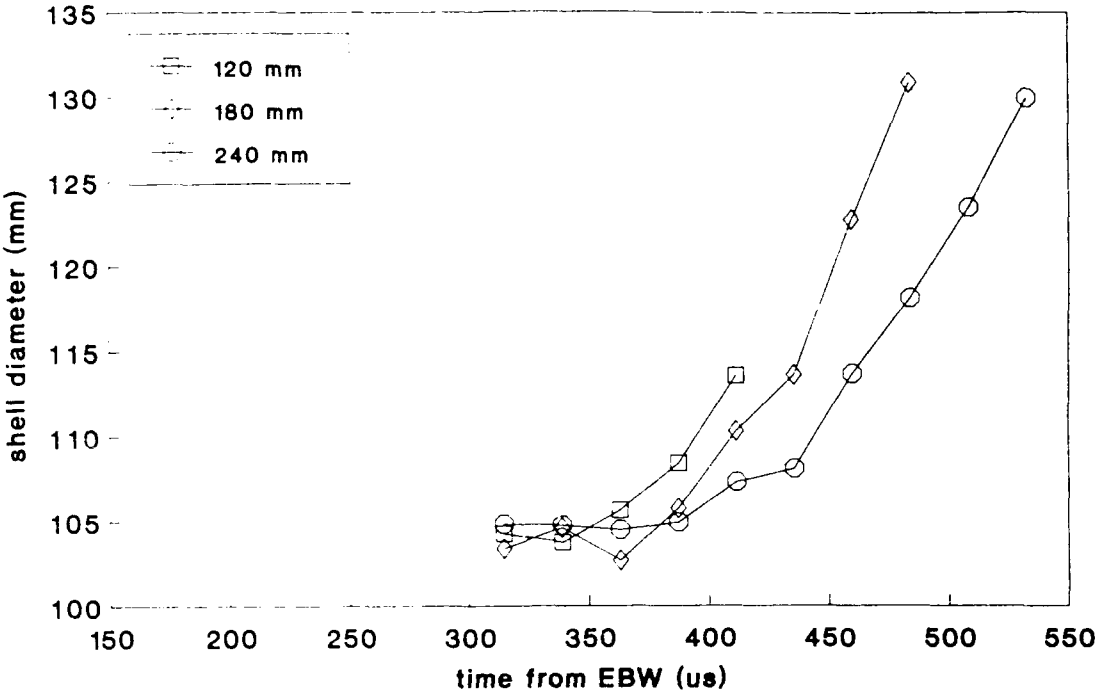

(a) Shot 1, Unplugged Shell

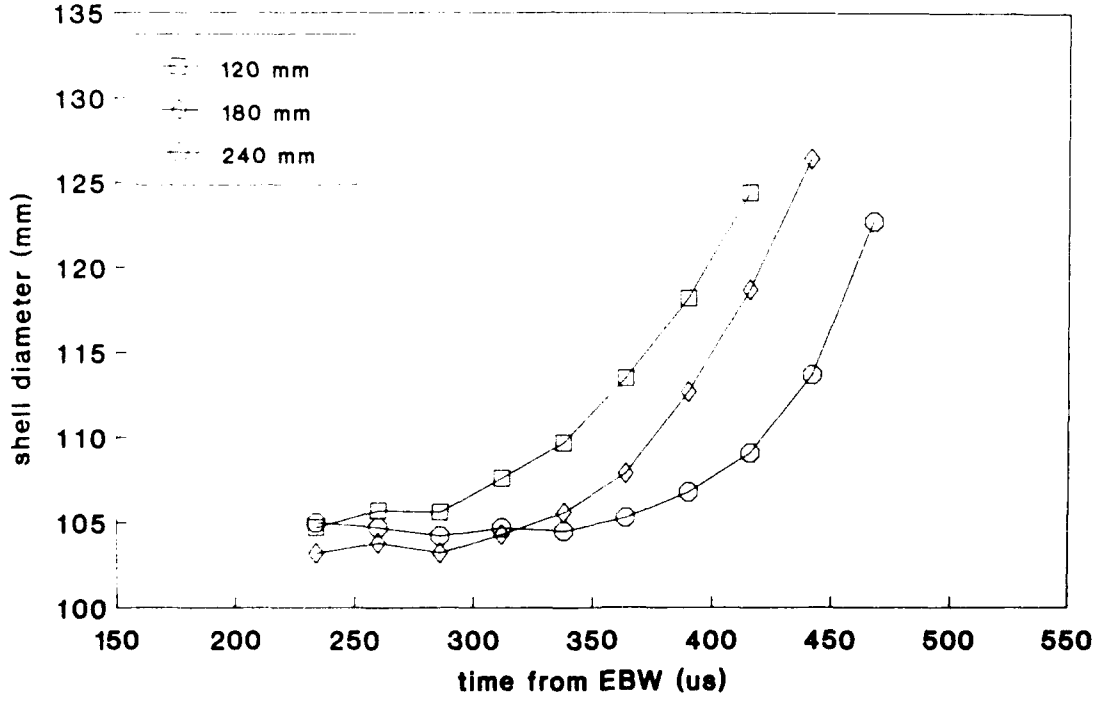

(b) Shot 2, Unplugged Shell

Figure 5: Plots of 105 mm shell diameter against time from the EBW firing pulse.

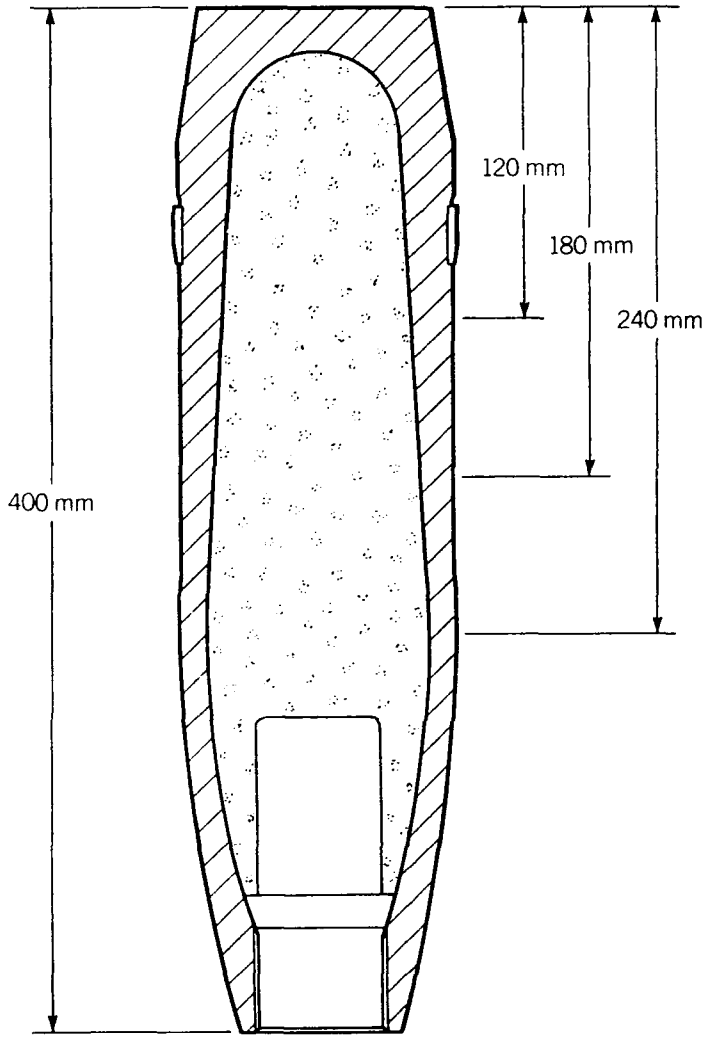

Figure 6: Points at which measurements of the shell diameter were made.

4.2 *Identification of Deflagration to Detonation Transitions*

The confinement presented by thick cased munitions such as the 105 mm shell (munition waist thickness 10 mm) encourages deflagration to detonation transitions (DDT) by holding partly reacting explosive fillings together. This occurred for example when subcritical shaped charge jets were fired through part of a Composition B filling in a 105 mm shell [19].

We have used high speed rotating prism photography to identify this process. Figure 7 shows the camera record of a Composition B 105 mm shell undergoing a DDT. Note the rapid belling out of the case at the nose immediately prior to being obscured by reaction products. In the plot in Figure 8 case expansion for Shot 5 at points 1 and 2 (see Figure 6) shows similar behaviour to that for Shots 1 and 4 and this is supported by the various event times for Shot 5 given in Table 1, i.e. deflagration reaction is occurring. However, point 3 for shot 5 in Figure 8 produced an estimated fragment velocity of 0.98 km/s (see Table 1) which is similar to the value of 1 km/s recorded from this part of the shell for a detonating Composition B filled 105 mm shell [18]. The conclusion that a DDT occurred is supported by the indentation produced in the witness block under the nose.

The reasons why a DDT occurred in Shot 5 are not clear. One possibility is that the shaped charge produced a poor quality jet that failed to completely penetrate the filling leaving heavily confined, vigorously reacting explosive.

Figure 7: Print of a section of the camera record showing the expansion of a 105 mm shell undergoing a deflagration to detonation transition.

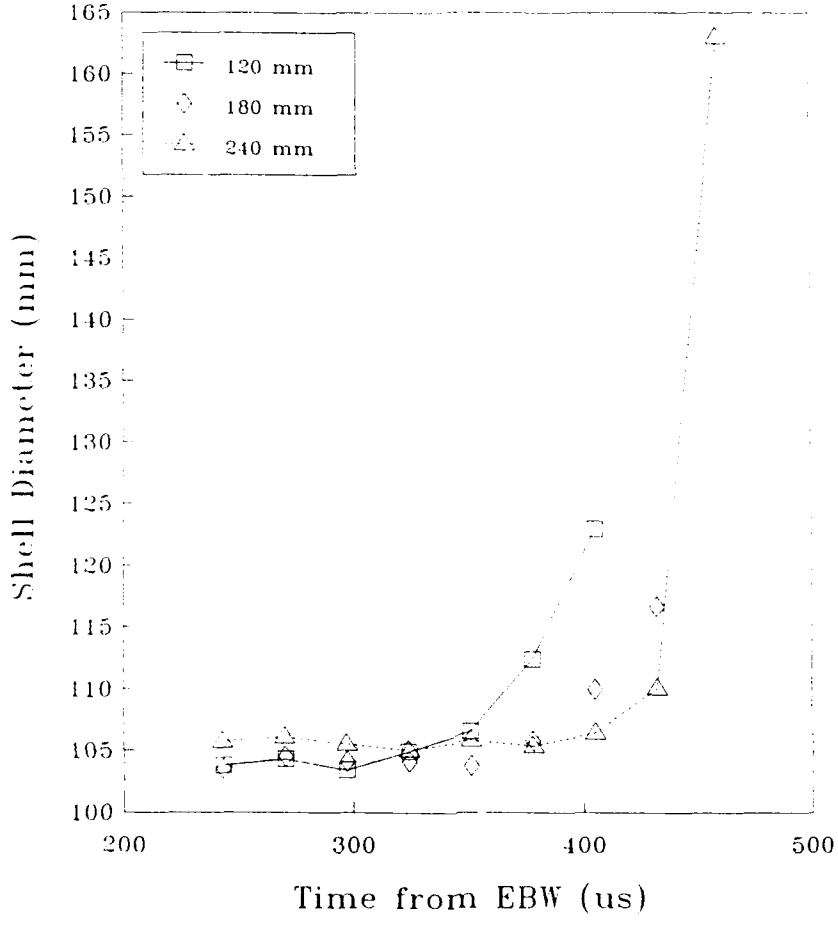

Figure 8: *Plot of 105 mm shell diameter against time from the EBW firing pulse.*

5. *Conclusions*

We have demonstrated that rotating prism high speed photography when run at framing rates near the upper limit of its range (i.e. 35 000 to 40 000 frames per second) can be used to characterise the deflagration of munitions. Parameters determined by this method included case expansion rate, initial fragment velocity, time to case burst, time to reaction from the nose end and the deflagration rate of the filling. The method was also able to identify the occurrence of a deflagration to detonation transition. Obscuration of the munition by products escaping from the fracturing case limited the extent of the measurements.

6. Acknowledgements

We wish to record our appreciation to Mrs L. McVay of MRL for assistance with the experiments and to the Officer Commanding and personnel of the Army Proof and Experimental Establishment, Graytown, Victoria for providing assistance and resources for the field firings.

7. References

1. Frey R.B., Watson, J., Gibbons, G., Boyle, V. and Lyman, O. (1990). *Proceedings of the Joint Government Industry Symposium on Insensitive Munitions Technology*, NSWC, White Oak, Maryland, US.

2. Stosz, M. (1987). Private Communication.

3. Frey, R.B. and Trimble, J.J. (1981). *Proceedings Seventh Symposium (International) on Detonation*, NSWC, MP 83-334.

4. Chick, M.C. and Bussell, T.J. Paper in course of publication.

5. Explosive Ordnance Disposal Procedures, Technical Manual. US Army, Navy, Air Force publication reference 60A-2-1-51, March 1981.

6. Chick, M.C., Bussell, T.J., Winter, P. and Learmonth, L.A. Unpublished information.

7. Chick, M.C. and Hatt, D. (1981). *Proceedings of the Seventh Symposium (International) on Detonation*, NSWC, MP82-334.

8. Chick, M., Bussell, T.J., Frey, R.B. and Bines, A. (1989). *Proceedings of the Ninth Symposium (International) on Detonation*, Portland, Oregon, US.

9. Burkoff, G., MacDougall, D., Pugh, E. and Taylor, G. (1948). *Journal of Applied Physics*, 19.

10. DiPersio, R. and Simon, J. (1964). Ballistic Research Laboratory Report No. 1542.

11. Allison, F.E. and Vitali, R. (1963). Ballistic Research Laboratory Report No. 1184.

12. Chou, P.C., Hirsch, E. and Walters, W. (1981).
Proceedings of Sixth International Symposium on Ballistics.

13. Chick, M.C., Bussell, T.J. and Frey, R.B. (1987).
Journal of Energetic Materials, 5.

14. Lee, K.J. (1983).
(MRL Technical Note MRL-TN-476). Maribyrnong, Vic.: Materials Research Laboratory.

15. Lee, K.J.
MRL Technical Note in course of publication. Maribyrnong, Vic.: Materials Research Laboratory.

16. Chick, M.C., Bussell, T.J. and McVay, L. (1990).
Proceedings of Twenty Fourth Department of Defence Explosives Safety Seminar, St Louis, Missouris, USA.

17. Chick, M.C., Bussell, T.J. and McVay, L.
Report in preparation.

18. Jenks, G.J., Lynch, B.J., Masinskas, J.J. and Oliver, J.D. (1972).
DSL Report 489, Confidential.

19. Chick, M.C., Bussell, T.J. and McVay, L. (1989).
Proceedings of 11th International Symposium on Ballistics, Brussels, Belgium.

20. Whalen, P.V. (1987).
Eglin Air Force Base Technical Report AD-TR-87-41. Limited Distribution.

DOCUMENT CONTROL DATA SHEET

REPORT NO.	AR NO.	REPORT SECURITY CLASSIFICATION
MRL-TR-91-43	AR-006-842	Unclassified

TITLE

Characterization of deflagrating munitions by rotating prism high speed photography

AUTHOR(S)
T.J. Kinsey
T.J. Bussell
M. Chick

CORPORATE AUTHOR
DSTO Materials Research Laboratory
PO Box 50
Ascot Vale Victoria 3032

REPORT DATE	TASK NO.	SPONSOR
August, 1992	DST 88/113	DSTO

FILE NO.	REFERENCES	PAGES
G6/4/8-4113	20	24

CLASSIFICATION/LIMITATION REVIEW DATE

CLASSIFICATION/RELEASE AUTHORITY
Chief, Explosive Ordnance Division

SECONDARY DISTRIBUTION

Approved for public release

ANNOUNCEMENT

Announcement of this report is unlimited

KEYWORDS

Sympathetic Detonation
Munitions Deflagration
High Speed Photography

ABSTRACT

We report on the use of a rotating prism high speed camera for determining the characteristics of a munition undergoing rapid deflagration in field experiments. The technique has been applied to study the controlled deflagration of Composition B filled 105 mm shell and 81 mm mortar bombs as representative thick and thin cased munitions respectively; however the report is mostly illustrated with results from the study on 105 mm shell. The deflagration event has been characterized in terms of case expansion rate, initial fragment velocity, time to case burst, time to reaction from the nose end and the deflagration rate of the filling. Products escaping from the fracturing case eventually obscured the image which limited the extent of the measurements.